

Dicke quantum spin glass of atoms and photons

Philipp Strack and Subir Sachdev

Department of Physics, Harvard University, Cambridge MA 02138

(Dated: September 13, 2011)

Recent studies of strongly interacting atoms and photons in optical cavities have rekindled interest in the Dicke model of atomic qubits coupled to discrete photon cavity modes. We study the multimode Dicke model with variable atom-photon couplings. We argue that a quantum spin glass phase can appear, with a random linear combination of the cavity modes superradiant. We compute spectral response functions across this quantum phase transition.

PACS numbers: 37.30.+i, 42.50.-p, 05.30.Rt, 75.10.Nr, 11.30.Qc

Introduction. Ultracold atoms in optical cavities have emerged as attractive new systems for studying strongly-interacting quantum many body systems. Photon exchange can mediate long-range interactions between the atomic degrees of freedom, and this opens up rich possibilities for correlated phases. In the celebrated atomic realizations of the superfluid-insulator quantum phase transition [1], the light field acts in a secular manner, creating a potential which traps the atoms in an optical lattice; consequently the atom-atom interactions are only on-site, and this limits the range of possible phases. In contrast, the seminal recent experiments of Baumann *et al.* [2, 3], realizing a supersolid phase, have long-range interactions mediated by active photon exchange.

Baumann *et al.* argued that their experiments could be described by the Dicke model, as in the proposal of Nagy *et al.* [4]. The Dicke model couples photons in a single cavity mode uniformly to N atomic two-level systems ('qubits'). In the limit $N \rightarrow \infty$, this model exhibits a phase transition [5–8] to a "superradiant" phase when the atom-photon coupling is strong enough. In terms of the qubits, the superradiant phase is a 'ferromagnet' which spontaneously breaks a global Ising symmetry, and so we refer to it as FM_{SR} .

Here we study extensions of the Dicke model to multiple photon cavity modes, and with non-uniform couplings between the atomic qubits and the photon modes. Multimode Dicke models have been studied earlier [5, 9–11], but were simplified by ignoring the variations in the atom-photon couplings. While this simplification is acceptable in the single cavity mode case, we argue here that qualitatively new physics emerges in the multimode case when the spatial variation is treated seriously. We argue that a quantum spin-glass (QSG) phase can emerge when the variations in the atom-photon couplings are large. We will describe quantum-critical dynamics associated with the onset of this spin glass order. Experimental realizations of the Dicke model have been discussed, for example, by Dimer *et al.* [12] using Raman transitions between multiple atomic levels; we expect that such schemes can be generalized to the multimode case. Such experiments would provide a unique realization of a quantum spin glass with long-range couplings, and provide a valuable testing ground for theories of quantum systems with strong interactions and disorder.

While our work was being completed, we learnt of the work

of Gopalakrishnan *et al.* [13] proposing a related realization of a spin glass in systems of atoms and photons.

Before describing our computations, we point out a key distinction between the transitions involving onset of FM_{SR} versus QSG order. In the single-mode Dicke model, all the qubits align in a common direction near the FM_{SR} phase, and can therefore be described by a collective spin of length $N/2$ which behaves classically in the limit of large N . Consequently, the dynamics near the phase transition can be described by classical equations of motion [14], and the single-mode Dicke model does not realize a *quantum* phase transition in the conventional sense of condensed matter physics. In contrast, we will argue here that the onset of QSG order in the multimode Dicke model has non-trivial quantum fluctuations even in the limit of large N , and the critical properties cannot be described by an effective classical model. Experimental studies are therefore of great interest.

Model. The Hamiltonian of the multimode Dicke model is

$$H = \sum_{i=1}^M \omega_i a_i^\dagger a_i + \frac{\Delta}{4} \sum_{\ell=1}^N \sigma_\ell^z + \sum_{\ell=1}^N \sum_{i=1}^M g_{i\ell} (a_i + a_i^\dagger) \sigma_\ell^x. \quad (1)$$

This describes N two-level atoms with level splitting $\Delta/2$ and M photon modes with frequencies ω_i coupled by an atom-photon coupling $g_{i\ell}$ which depends on the photon (i) and atom (ℓ) number. a_i^\dagger, a_i are bosonic creation and annihilation operators, respectively, fulfilling canonical commutation relations. $\sigma_\ell^{x,z}$ are spin-1/2 operators with Pauli matrix representation.

In the single-mode, large photon wavelength case, we have $M = 1$, $\omega_i = \omega_0$, and $g_{i\ell} = g/\sqrt{N}$ and the model can be solved exactly in the $N \rightarrow \infty$ limit [5, 6]. At zero temperature, there is a continuous phase transition between a paramagnetic phase (PM) and a superradiant ferromagnetic phase (FM_{SR}) at $g = g_c = \sqrt{\Delta\omega_0}/8$ at which the Ising symmetry (a, σ_x) $\rightarrow (-a, -\sigma_x)$, is spontaneously broken.

For the multimode Dicke model, it is useful to integrate out the photon degrees of freedom in a path-integral representation. Then the qubits are described by a Hamiltonian similar to the Ising model in a transverse field,

$$H_{\text{eff}} = \frac{\Delta}{4} \sum_{\ell=1}^N \sigma_\ell^z - \frac{1}{2} \sum_{\ell m} J_{\ell m} \sigma_\ell^x \sigma_m^x, \quad (2)$$

The exchange interactions $J_{\ell m}$ are mediated by the photons

and have a frequency dependence associated with the photon frequencies ω_i ; thus Eq. (2) is to be understood as an action appearing in an imaginary time path-integral summing over time-histories of the qubits. We have the long-range exchanges

$$J_{\ell m}(\Omega) = \sum_{i=1}^M \frac{2g_{i\ell}g_{im}\omega_i}{\Omega^2 + \omega_i^2}, \quad (3)$$

where Ω is the imaginary frequency of the qubits in the path integral. If we ignore the frequency dependence in Eq. (3), the $J_{\ell m}$ have a structure similar to the Hopfield model of associative memory [15], with M ‘patterns’ $g_{i\ell}$. For M small, it is expected that such a model can have M possible superradiant ground states with FM_{SR} order $\langle \sigma_\ell^x \rangle \propto g_{i\ell}$, $i = 1 \dots M$. In the spin-glass literature, these are the Mattis states which are “good” memories of the patterns g [15]. The critical properties of the onset of any of these FM_{SR} states should be similar to those of the single mode Dicke model.

Our interest in the present paper will be limited to larger values of M , where the summation in Eq. (3) can be viewed as a sum over M random numbers. By the central limit theorem, the distribution of $J_{\ell m}(\Omega)$ is Gaussian, and is characterized by its mean and variance. We take these to have the form

$$\begin{aligned} \langle J_{\ell m}(\Omega) \rangle &= J_0(\Omega)/N \\ \langle \delta J_{\ell m}(\Omega) \delta J_{\ell' m'}(\Omega') \rangle &= (\delta_{\ell\ell'} \delta_{mm'} + \delta_{m\ell'} \delta_{\ell m'}) K(\Omega, \Omega')/N, \end{aligned} \quad (4)$$

where $\delta J_{\ell m}$ is the variation from the mean value. We have assumed couplings between different sites are uncorrelated, and this will allow an exact solution in the $N \rightarrow \infty$ limit, modulo an innocuous softening of the fixed length constraint on the Ising variable [16, 17]. We will allow *arbitrary* frequency dependencies in $J_0(\Omega)$ and $K(\Omega, \Omega')$. The factors of N ensure an interesting $N \rightarrow \infty$ limit [18]. In principle, we can use the methods of Ref. [15] to extend our analysis to models in which the $g_{i\ell}$ rather than the $J_{\ell m}$ are taken as independent random variables: such an analysis will be especially important at smaller values of M . However, we will not discuss this here.

Key results. We will show below that, in the limit of large N , the results depend only upon $J_0(\Omega = 0)$ and $K(\Omega, -\Omega)$. Here, we will display the phase diagram and spectral response functions for the simple choices $K(\Omega, -\Omega) \equiv J^2(\Omega)$ with

$$J(\Omega) = 2t^2\omega_0/(\Omega^2 + \omega_0^2), \quad (5)$$

and $J_0(0) = 2g^2/\omega_0$.

In Fig. 1, we depict the ground state phase diagram; a related phase diagram in a condensed matter context was obtained in Ref. 19. All phase transitions are continuous and the respective phase boundaries merge in a bicritical point at $(t_{bc}^2 = 0.086, g_{bc}^2 = t_{bc}^2)$.

The intersection of the PM-FM_{SR} phase boundary with the vertical axis at $t^2 = 0$ corresponds to the phase transition in the single mode Dicke model without disorder [7, 12]. In this case, a number of analytical results can be obtained from Eq.

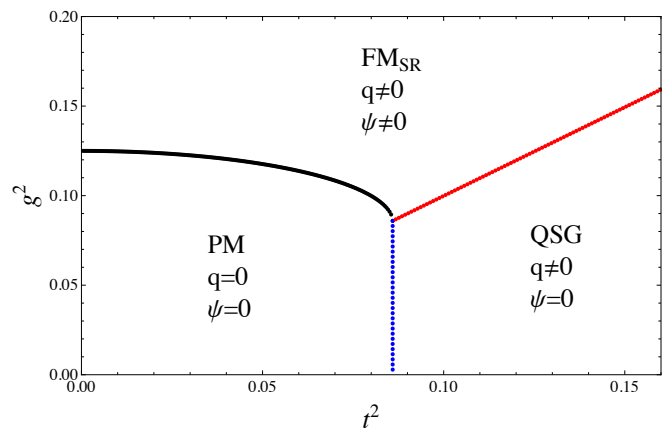


FIG. 1: (Color online) Zero-temperature phase diagram for $\omega_0 = 1$, $\Delta = 1$ computed from Eq. (10). PM means paramagnet, FM_{SR} superradiant ferromagnet, and QSG quantum spin glass. q is the Edwards-Anderson order parameter and ψ the ferromagnetic order parameter or atomic population inversion.

(10), in agreement with the earlier work. The critical atom-photon coupling is $g_c^2 = \Delta\omega_0/8$ and the local σ^x spin susceptibility in the FM_{SR} phase is (for imaginary frequencies)

$$Q_{t^2=0}^{aa}(\Omega) = \frac{\Delta}{\Omega^2 + 2\Delta g^2/\omega_0} + \psi^2 2\pi\delta(\Omega). \quad (6)$$

This encodes the superradiance in the zero frequency delta function contribution depicted in Fig. 2, whose weight is proportional to the ferromagnetic order parameter ψ . However, note that away from the zero frequency delta function, there is a spectral gap, and the remaining spectral weight is a delta function at frequency $\sqrt{2\Delta g^2/\omega_0}$.

Upon introducing small disorder (with $t \neq 0$), as long as we remain in the FM_{SR} phase, the zero frequency delta function and spectral gap survive, although the higher frequency spectral weight changes, as shown in Fig. 2. This spectral gap is present across the phase transition from the FM_{SR} phase to the PM phase. Thus all the low energy fluctuations in the critical theory for this transition are restricted to the zero frequency delta function, which can be described in classical theory for the spins: this is the reason this transition is more properly considered as a *classical* phase transition.

For a sufficiently large value of t^2 , the system undergoes a quantum phase transition to the QSG ground state. In contrast to the PM-FM_{SR} transition, at the QSG transition, and in the entire QSG phase, there is spectral weight at a continuum of frequencies reaching zero (see Fig. 3). Thus the onset of QSG order from the PM phase is a *quantum* phase transition, whose universality class was described in Ref. 17.

We also note that in all phases, while the spectral function has a universal form at low frequencies, its high frequency behavior is strongly dependent upon the forms of $J_0(\Omega)$ and $J(\Omega)$. For the forms in Eq. (5), the spectral function is suppressed to zero at $\Omega = \omega_0$.

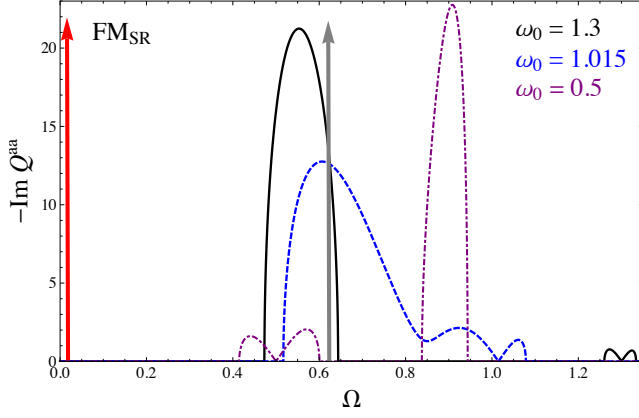


FIG. 2: (Color online) Spectral function in the FM_{SR} phase for various photon frequencies and $t^2 = 0.025$, $g^2 = 0.2$, $\Delta = 1$. The red arrow at $\Omega = 0$ illustrates the delta function contribution with weight proportional to $q \sim \psi$ from Eqs. (11,12). The value of the gap is given above Eq. (12). For the Dicke model without disorder ($t^2 = 0$), the spectral function following from Eq. (6) consists of nothing but two delta functions: the red arrow at $\Omega = 0$ and the grey arrow at $\Omega = g\sqrt{2\Delta/\omega_0}$ (plotted for $\omega_0 = 1.015$).

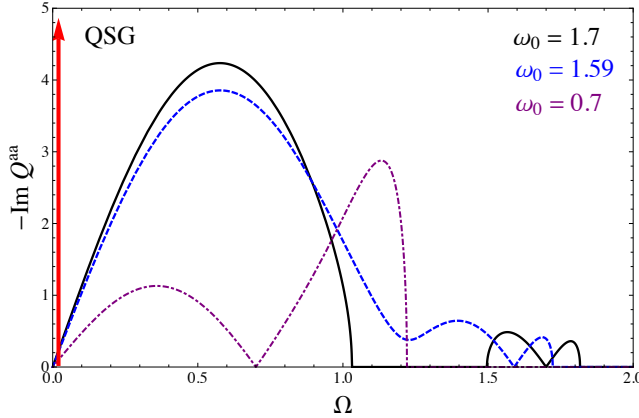


FIG. 3: (Color online) Spectral function in the QSG phase for various photon frequencies and $t^2 = 0.175$, $g^2 = 0.05$, $\Delta = 1$. The red arrow at $\Omega = 0$ illustrates the delta function contribution with weight proportional to q_{QSG} from Eqs. (11,13).

Details of the calculation. As discussed in Refs. 16, 17, each Ising qubit, with on-site gap $\Delta/2$, is conveniently represented by fluctuations of a non-linear oscillator $\phi_\ell(\tau)$ (τ is imaginary time) which obeys a unit-length constraint. Their action at temperature T is then

$$S_0[\phi, \lambda] = \frac{1}{2\Delta} \sum_{\ell=1}^N \int_0^{1/T} d\tau [(\partial_\tau \phi_\ell)^2 + i\lambda_\ell (\phi_\ell^2 - 1)] \quad (7)$$

where τ is imaginary time, and the λ_ℓ are Lagrange multipliers which impose the constraints. The *only* approximation of this paper is to replace the λ_ℓ by their saddle-point value, $i\lambda_\ell = \lambda$, and to ignore their fluctuations. For decoupled oscillators, this saddle-point value is $\lambda = \Delta^2/4$, the ϕ susceptibility is

$\Delta/(\Omega^2 + \Delta^2/4)$, and the resulting gap, $\Delta/2$, has been matched to that of the Ising spin.

The interactions between the qubits are accounted for as before [16]: we introduce replicas $a = 1 \dots n$, average over the $J_{\ell m}$ using Eq. (4), decouple the resulting two- ϕ coupling by Hubbard-Stratonovich transformation using a ferromagnetic order parameter $\Psi^a(\Omega)$, and the four- ϕ coupling by the bilocal field $Q^{ab}(\Omega_1, \Omega_2)$ [17] (the Ω are Matsubara frequencies). The complete action is

$$\begin{aligned} S = & \sum_a S_0[\phi^a, \lambda^a] + T \sum_{a,\Omega} J_0(\Omega) \left[\frac{N}{2} |\Psi^a(\Omega)|^2 \right. \\ & - \Psi^a(-\Omega) \sum_{\ell=1}^N \phi_\ell^a(\Omega) \left. + \frac{T^2}{2} \sum_{a,b,\Omega,\Omega'} K(\Omega, \Omega') \left[\frac{N}{2} |Q^{ab}(\Omega, \Omega')|^2 \right. \right. \\ & \left. \left. - Q^{ab}(-\Omega, -\Omega') \sum_{\ell=1}^N \phi_\ell^a(\Omega) \phi_\ell^b(\Omega') \right] \right]. \quad (8) \end{aligned}$$

Now we perform the Gaussian integral over the ϕ_ℓ : the resulting action has a prefactor of N , and so can be replaced by its saddle-point value. By time-translational invariance, the saddle-point values of the fields can only have the following frequency dependence

$$\begin{aligned} \Psi^a(\Omega) &= (\delta_{\Omega,0}/T) \psi \\ Q^{ab}(\Omega, \Omega') &= (\delta_{\Omega+\Omega',0}/T) [\chi(\Omega)\delta^{ab} + (\delta_{\Omega,0}/T) q], \quad (9) \end{aligned}$$

and we take $\lambda^a = \lambda$. We have assumed replica symmetry for the Edwards-Anderson order parameter q because our interest will be limited here to $T = 0$ where there is no replica symmetry breaking [17]. Now the values of the ferromagnetic moment ψ , the spin susceptibility $\chi(\Omega)$, q , and λ have to be determined by optimizing the free energy. The latter is obtained by inserting Eq. (9) in Eq. (8); after taking the replica limit $n \rightarrow 0$, we have the free energy per site

$$\begin{aligned} \mathcal{F} = & \frac{J_0(0)\psi^2}{2} + \frac{T}{4} \sum_{\Omega} K(\Omega, -\Omega) |\chi(\Omega)|^2 + \frac{1}{2} K(0,0) \chi(0) q \\ & + \frac{T}{2} \sum_{\Omega} \ln \left(\frac{(\Omega^2 + \lambda)}{\Delta} - K(\Omega, -\Omega) \chi(\Omega) \right) - \frac{\lambda}{2\Delta} \\ & - \frac{1}{2} \left[\frac{K(0,0)q + J_0^2(0)\psi^2}{\lambda/\Delta - K(0,0)\chi(0)} \right]. \quad (10) \end{aligned}$$

Note that this free energy depends only upon $J_0(0)$ and $K(\Omega, -\Omega)$, as claimed earlier. Our results described in Eq. (6) and Figs. 1-3 are derived from a set of coupled saddle-point equations obtained from varying Eq. (10) with respect to $\chi(\Omega)$, q , ψ , and λ for every Ω . Subsequently we let $T \rightarrow 0$.

For the choices for $K(\Omega, -\Omega)$ and $J_0(0)$ of Eq. (5), the spectral function plotted in figures 2,3 is given by the expression:

$$\begin{aligned} -\text{Im} [Q^{aa}(i\Omega \rightarrow \Omega + i0_+)] = & \quad (11) \\ & \frac{|\omega_0^2 - \Omega^2| \sqrt{16\Delta^2 t^4 \omega_0^2 - (\lambda - \Omega^2)^2 (\omega_0^2 - \Omega^2)^2}}{8\Delta t^4 \omega_0^2} + q 2\pi\delta(\Omega). \end{aligned}$$

The first term is non-zero only for frequencies Ω so that the expression underneath the square-root is positive. The value of the Lagrange multiplier in the FM_{SR} is pinned to $\lambda_{\text{FM}} = \Delta(J_0(0) + K(0,0)/J_0(0))$. The value of the gap in Fig. 2 is

$\sqrt{\frac{1}{2} \left(\lambda_{\text{FM}} + \omega_0^2 - \sqrt{16\Delta t^2 \omega_0 + (\lambda_{\text{FM}} - \omega_0^2)^2} \right)}$. This expression equates to zero in the gapless QSG phase shown in Fig. 3, where $\lambda_{\text{QSG}} = 2\Delta \sqrt{K(0,0)}$. This gap vanishes logarithmically faster than $(t^2 - t_c^2)$ when approaching the QSG phase boundary due to the square-root behavior of the spectral weight [16, 20].

The ferromagnetic moment obtains as

$$\psi^2 = \frac{J_0^2(0) - K(0,0)}{J_0^2(0)} \left(1 - \int_{-\infty}^{\infty} \frac{d\Omega}{2\pi} \chi(\Omega) \Big|_{\lambda=\lambda_{\text{FM}}} \right), \quad (12)$$

and ψ vanishes continuously at the FM_{SR} -QSG phase boundary (at which $J_0(0) = \sqrt{K(0,0)}$) with exponent $\beta_{\text{FM}} = 0.5$. Note that the Edwards-Anderson order parameter q is continuous across this transition and in the QSG phase given by:

$$q_{\text{QSG}} = 1 - \int_{-\infty}^{\infty} \frac{d\Omega}{2\pi} \chi(\Omega) \Big|_{\lambda=\lambda_{\text{QSG}}}. \quad (13)$$

As expected, one obtains numerically $\beta_{\text{QSG}} = 1.0 = 2\beta_{\text{FM}}$.

Outlook. Our analysis here has been limited to a closed Dicke model, and the phase transition exhibited by its internal quantum dynamics. Implementation in quantum optics requires consideration of input and output from the photon modes, and decay into photons transverse to the cavity. We leave a complete analyses of these effects to future work. However, we note a similarity of the decay effects to those in theories of *metallic* spin glass [21], in which the spin qubits were coupled to a ‘‘reservoir’’ of continuum spin excitations near the Fermi surface. This coupling led a damping term in the dynamics of each spin, but did not significantly modify the spin-spin interactions responsible for the spin glass phase. Similarly, for an ‘open’ Dicke model, decay into photons outside the cavity will introduce various damping terms *e.g.* a $\kappa|\Omega|$ term in the denominator of Eq. (3), where κ is a decay rate. As in the previous analyses [21], we expect that the quantum spin glass transition will survive in the presence of damping, although there will be some changes to the critical properties of the phase transition.

Another important topic for future research is the real time dynamics of the spin glass phase. As in other spin glasses, we expect slow glassy dynamics, along with memory and

aging effects. Observations of such effects in quantum optic systems would be remarkable. Moreover, as we have argued here, the theoretical models for the spin glass physics have long-range interactions, and this makes them analytically tractable. We therefore have prospects for a quantitative confrontation between theory and experiment in a glassy regime, something which has eluded other experimental realizations of spin glasses.

We thank J. Bhaseen, T. Esslinger, J. Keeling, M. Punk, P. Zoller, and especially J. Simon for useful discussions. This research was supported by the DFG under grant Str 1176/1-1 and by the NSF under Grant DMR-1103860.

-
- [1] M. Greiner, O. Mandel, T. Esslinger, T. W. Hänsch, and I. Bloch, *Nature* **415**, 39 (2002).
 - [2] K. Baumann, C. Guerlin, F. Brennecke, and T. Esslinger, *Nature* **464**, 1301 (2010).
 - [3] K. Baumann, R. Mottl, F. Brennecke, and T. Esslinger, arXiv:1105.0426 (2011).
 - [4] D. Nagy, G. Kónya, G. Szirmai, and P. Domokos, *Phys. Rev. Lett.* **104**, 130401 (2010).
 - [5] K. Hepp, and E. H. Lieb, *Annals of Physics* **76**, 360, (1973).
 - [6] Y. K. Wang, and F. T. Hioe, *Phys. Rev. A* **7**, 3 (1973).
 - [7] C. Emary, and T. Brandes, *Phys. Rev. E* **67**, 066203 (2003).
 - [8] J. Ye, and C. Zhang, *Phys. Rev. A* **84**, 023840 (2011).
 - [9] V. I. Emeljanov and Yu. L. Klimontovich, *Phys. Lett.* **59**, 366 (1976).
 - [10] B. V. Thompson, *J. Phys. A* **10**, 89 (1977); *ibid.* **10**, L179 (1977).
 - [11] D. Tolkunov, and D. Solenov, *Phys. Rev. B* **75**, 024402 (2007).
 - [12] F. Dimer, B. Estienne, A. S. Parkins, and H. J. Carmichael, *Phys. Rev. A* **75**, 013804 (2007).
 - [13] S. Gopalakrishnan, B. L. Lev, and P. M. Goldbart, arXiv:1108.1400 (2011).
 - [14] J. Keeling, M. J. Bhaseen, and B. D. Simons, *Phys. Rev. Lett.* **105**, 043001 (2010).
 - [15] D. J. Amit, H. Gutfreund, and H. Sompolinsky, *Phys. Rev. Lett.* **55**, 14 (1985).
 - [16] J. Ye, S. Sachdev, and N. Read, *Phys. Rev. Lett.* **70**, 25 (1993).
 - [17] N. Read, S. Sachdev, and J. Ye, *Phys. Rev. B* **52**, 1 (1995).
 - [18] K. H. Fischer, and J. A. Hertz, *Spin Glasses* (Cambridge Univ. Press, Cambridge, 1991).
 - [19] D. Dalidovich, and P. Phillips, *Phys. Rev. B* **59**, 18 (1999).
 - [20] J. Miller, and D. A. Huse, *Phys. Rev. Lett.* **70**, 20 (1993).
 - [21] S. Sachdev, N. Read, and R. Oppermann, *Phys. Rev. B* **52**, 10286 (1995).